On the Search of the Optical Counterparts of Binary Neutron Star Merge with the Large Synoptic Survey Telescope

Lai Chun Ming, Anderson

Mentors:
Dr. Jeff Tseng and Dr. Rahul Biswas

2019-09-28

Abstract

The registration of LIGO's GW170817 as a binary neutron star(BNS) merging event and the successful follow-up on its electromagnetic counterpart revealed the power and potential of multi-messenger astronomy. With the refining efficiency and sensitivity on detectors, it is believed that next decade's instruments are sufficient for the discovery of more BNS merge events and the Large Synoptic Survey Telescope(LSST) would be one of the candidate to follow up the optical transient. In this report, a brief introduction on the theory of the optical counterpart will be given, followed by a presentation on the work of evaluating how a LSST observation detects optical transients from BNS merge.

1 Introduction

1.1 The Discovery of GW170817

On 17 August, 2017, the Fermi Gamma-ray Burst Monitor reported a gamma ray burst(GRB). 6 minutes later, a gravitational wave signal was reported firstly by the Laser Interferometer Gravitational-wave Observatory(LIGO) after an analysis on Hanford's data(now called GW170817A)[1]. With the detection on the same event from Virgo, various parameters had been estimated, including a coalescence time 2 seconds before the GRB signal(now called GRB 170817A), a localization area of 31 square degree which overlaps with the GRB 170817A one(figure 1), a luminosity distance of 40 Mpc and binary masses of 1.36-2.66 and 0.86-1.36 solar mass.

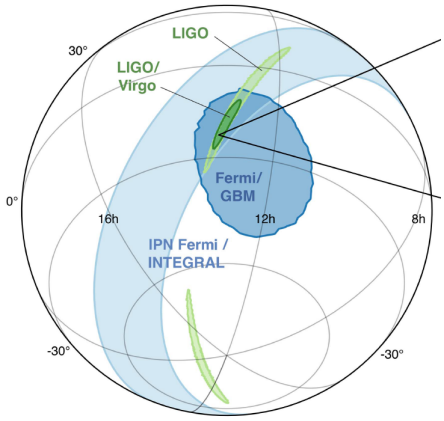

Figure 1: The localization region of the GRB 170817A detected by Fermi GRB monitor, LIGO's detection and LIGO/Virgo's detection from [1]. As one can see from the figure, LIGO/Virgo's inferred localization(in deep green) completely lies within the GRB localization region(blue). The short time interval between two events provided hint for scientist to search for the optical counterpart. On the other hand, one might notice a three-point localization using LIGO and Virgo produces a much smaller localization area than LIGO's detection itself.

These coincidences between two events suggested a binary neutron star merge, in couple with a possibly-detected optical transients. Therefore, swift follow-up on the search of electromagnetic counterpart(EM counterpart) had been made, resulting a successful discovery of a bright optical signal(AT 2017gfo) 11 hours later, which resided in NGC4993, one of the galaxies within the localization region.

1.2 Challenges in Optical Follow-up on Gravitational Wave Enevts

Although GW170817A symbolises a success in multi-messenger astronomy, it is the only event that can be detected in both gravitational wave (GW) and EM wave until now. GW170817A is regarded to be a fortunate case because of the exceptional high difficulty to search for the optical part of a BNS merge, which could be concluded into following reasons.

To begin with, the intrinsic nature of the signal determines the likelihood and number of detectable candidates. For a gravitational signal strong enough to be detected by LIGO/Virgo, it has to originate from the merge of compact objects, and the type of the merger can be determined from the chirp mass. However, for an optical signal with a certain brightness, there are millions of candidates over a localization region of few tenth square degree which carries similar apparent magnitude, together with a classification ranging from a few days to 2 weeks. Hence, an optical follow-up on optical transient is not as efficient as the gravitational wave one.

Next, the magnitude of optical counterpart strongly depends the propagation environment between the merger and Earth. For example, absorption and scattering happen when EM signal passing through interstellar dusts. Hence, apart from the luminosity distance, the brightness of the signal would also drop with the extent on interstellar and host galaxy extinction. Moreover, if the merger lies on milky way's galactic plane, there is impossible to differentiate the optical counterpart from the bright milky way background. As a result, true optical signals are usually veiled by high signal-to-noise ratio(SNR) and uable to trigger any detection system. Anal-

ogous arguments has been made in [2].

Lastly, local conditions impose criteria for an observation in optical band. If there is a poor weather in the following week of a BNS merge event, it would be impossible to do telescope observation and look for optical transients. Furthermore, one has to avoid daytime to search for an optical signal. Geographic restrictions including a ground-based telescope located in southern hemisphere unable to capture a northern localization region.

1.3 The Large Synoptic Survey Telescope

In regard to various obstacles that arise from detecting the optical transient of a BNS merge. There is a need for new telescope with unprecedented sensitivity, coverage over the sky and amount of data transport. The Large Synoptic Survey Telescope(LSST) is considered to be a potential candidate that is capable with the job. The ground-based telescope is located in Chile and expected to operate in 2022. It features a 9.6 square degree field of view(FOV) and a lens with 8.4 metre diameter. Images will be captured with a 3.2 Gigapixel camera and sent to the world in a real-time manner.

A combination of LSST specifications makes the telescope able to pick up a large region over the sky with a 5-sigma depth up to 24.3 apparent magnitude in a single capture, while all the detailed features including galaxies and any optical transients can be clearly differentiate by the high-resolution camera. The real time data transport flavors one to put the transient data into any analysing tools instantly. To sum up, LSST provides the necessity for a search of optical signal from BNS merge.

LSST is equipped with differnt observation proposals[3], including a major Wide-Fast Deep(WFD) one, a minor Deep-Drilling Field proposal and other strategies. For a 10 year survey, WFD constitutes 85% of the total time, monitoring one-fourth of the whole sky by repeating visits over 10 years. For DDF, only several sites were selected, but they are studied with longer exposure time and contribute 10-25% of the total time. The rest of the time are composed by other strategies that are made to study specified objects. Thus, by combining LSST with a suitable proposal, it is believed that followup on optical counterparts from LIGO-detected BNS merge could be effectively executed.

2 Theory

2.1 Mechanisms for Ejecta Formation

For a BNS merge, there are no optical radiations emitted from the merger itself. Therefore, the optical counterpart is actually originated from the ejecta of the merger. There are mainly three kinds of ejecta proposes by literature, each of them emerges in subsequent timescale. The first one is the tidal ejecta, which is formed due to the tidal force between the merging neutron stars during the pre-merge sequence, due to their high mass, the strong tidal force tears a small fraction of mass from neutron stars. According to Rosswrog and Hotokezaka, the tidal ejecta consists of 10^{-2} to 10^{-4} solar mass which increases with the mass ratio, or equivalently, the eccentricity of the orbit[4, 5]. As it is likely to retain the composition of a neutron star, it has a small electron fraction(0.1-0.2) distributed along the merge plane.

Next kind of ejecta emanates from the shockwave generated by the merge, when two neutron stars merge together, another portion of neutron star material is thrown out along the rotational axis at pole and powered by a shockwave. As mentioned in Wanajo[6], shock heating and weak interaction effect in polar ejecta, which raise the electron fraction up to 0.25 or beyond. theory suggests a similar mass as the tidal ejecta but varies with the remnant and the radius of the posterior hyper-massive neutron star.

At the post-merging sequence, the circumstellar remnant accretes into the hyper-massive neutron star, the accretion disk is then heated and

throwing away material in the form of isotropic disk wind, which is the third kind of ejecta. Apart from keeping the original composition in neutron star, the accretion heating fosters a wide spectrum of radioactive reaction which enriches an electron fraction ranging from 0.1 to 0.4[7]. The outflow, although consists of a solar mass up to 0.07, is relatively slow compare to other two kinds of ejecta. Due to its isotropy, it is considered to be a promising source of the optical transient in company with the BNS merge.

Note that above ejecta mechanisms have assumed a BNS merge that the remaining compact object is able to support itself to be a hypermassive neutron star for a certain period. A summary on the ejecta mechanism is illustrated in figure 2.

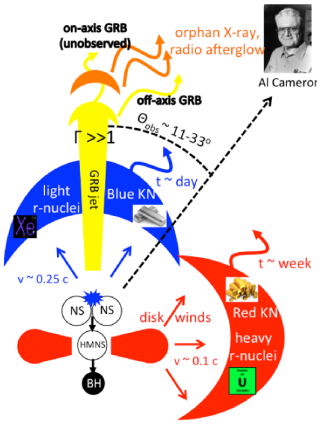

Figure 2: A figure from[7], it consists of the polar ejecta and the disk wind, By the time two neutron stars merge, materials are thrown away in polar direction and powered by the shockwave which makes their photon diffusion SED peaks at bluer wavelength(section 2.2). Supposing a posterior hyper-massive neutron star(HMNS) exists, disk wind due to the accretion of ejecta will generate the second optical transients with SED peaks at redder wavelength. The θ_obs is the observation angle in AT2017gfo

2.2 Origin of photons and Thermalization of Ejectas

The high-neutron-density ejecta and massive heating creates an environment which flavors an unfamiliar rapid neutron capture process(r-process)[8]. As described in equation 1, energetic neutrons are fused into larger nucleus at excited state, followed by a transition to ground state by emitting photons.

$$ {}^{1}_{0}n + {}^{a}_{b}X \rightarrow {}^{a+1}_{b}X^{*} \rightarrow {}^{a+1}_{b}X + \gamma - (1) $$

This is the birthplace of the EM counterpart. On the other hand, r-process is believed to be able to bring the final mass of the nucleus up to the range of lanthanides. These heavy nucleus remains unstable due to the dominating neutron ratio, leading subsequent beta decays(equation 2). Therefore, free electron density begins to rise because of the synthesized product in beta decay.

$$ {}^{a}_{b}X \rightarrow {}^{a}_{b+1}X + e^{-} + \overline{\nu_e} - (2) $$

Nevertheless, photons from r-process still possessing high energy and they are not going to lie on the optical band. Therefore, thermalization including absorption and electron scattering takes place when photons diffuse to the outermost layer of the ejecta. As the thermal equilibrium reaches and the ejecta become 'transparent', escaped photons compose a spectral energy distribution(SED) which that peaks at optical band. A rough estimation had been made by Kasen in 2013 to show the thermalization would be dominated by bound-bound absorption[8]. In other words, the SED of the optical transient closely relates to the chemical composition of the ejecta.

Because of the varying physical properties of three ejecta(velocity, electron fraction etc.), different SEDs are expected. The tidal ejecta's SED would peak at redder wavelength due to its low electron fraction. In contrast, polar ejecta gives a bluer SED regarding a higher electron fraction. While for disk wind, a superposition of both blue and redder ejecta is expected. Assorted models had been suggested, comprising single-component model with heavy r-process nucleus only[9], two-component model with light and heavy lanthanides[10] and models with parametrised opacities instead of detail calculation on the atomic configurations[11, 12].

2.3 Photon diffusion timescale and peak magnitude

To develop an observation strategy with BNS merge optical counterpart, there is necessity to estimate the photon diffusion timescale and peak luminosity. These two important parameters set the limit on the epoch between observations and the sensitivity of the telescope. According to Arnett 1982's derivation[13, 14], one can begin with the first law of thermodynamics(equation 3):

$$\dot{E} + P\dot{V} = -\frac{\partial L}{\partial m} + \epsilon - (3)$$

Where $\dot{E}$ is the rate of internal energy change per unit mass, P is pressure, $\dot{V}$ is rate of change of volume, L is luminosity, m is the mass of the ejecta and ϵ is the decay heating energy rate per unit mass. To keep the simplicity, we assume the ejecta as a spherical ejecta with isotropic expansion(equation 4):

$$R(t) = R(0) + v_{sc}t - (4)$$

Where Rt is the outermost radius of the ejecta at time t and v_{sc} is the expansion velocity. For an analytical solution, we parametrise the temperature T and volume V of the ejecta:

$$\begin{cases} \mathrm{V(r,t)} = \mathrm{V(0,0)}\left[\frac{R(t)}{R(0)}\right]^3 - (5a) \\ \mathrm{T(r,t)}^4 = \psi(r)\phi(t)T(0,0)^4\left(\frac{R(0)}{R(t)}\right)^4 - (5b) \end{cases}$$

Notice that Arnett's derivation demands a stationary state on temperature by separating it into radial part $\psi(r)$ and time part $\phi(t)$.

After a long manipulation of above equations and stellar structure equations, we arrive an expression on the typical photon diffusion timescale τ_0(equation 6):

$$\tau_0 = \frac{\kappa M}{R(0)} - (6)$$

In this expression, κ is the mean opacity of the ejecta which encodes the information of ejecta composition. M is the total ejecta mass and β is a constant. From here, we adopt the estimation mentioned in Metzger 2010 by substituting tau_0 with free expansion relation(equation 4) and input typical parameters including $v_s c = 0.1c$, $m = 0.01 solarmass$, $\kappa = 0.1 cm^2 g^{-1}$ and $\beta = 0.07$, we can calculate the peak time scale t_p afterwards[15]:

$$t_p = 0.5 days$$

Proceeding the discussion in Metzger's 2010 paper, the energy releases due to radioactive heating Q is a tiny fraction of the rest mass energy of the ejecta:

$$Q \approx fMc^2, f = 10^{-6} - (6)$$

Eventually, the peak luminosity is estimated to be:

$$L_p = \frac{Q}{t_p} \approx 5 \times 10^{41} ergs^{-1}$$

It is known that a typical nova has a luminosity of the order of $1 \times 10^{38} ergs^{-1}$, while $10^{-2\sim-3}$ to that of a typical supernova(SN). Therefore, the optical transient powered by r-process in the BNS merge ejecta is often called a 'Kilonova'(KN)

2.4 Scientific Value of Studying the Optical Transient

The properties of BNS merge ejecta and some parameters of KN reveal the significance of understanding KN with practical detection. First of all, the tidal ejecta is directly constituted by neutron star material, while the disk wind is full of r-process products. Their compositions are reflected in the optical SED. Therefore, spectroscopy on the lightcurve of KN could enhance our understand of the oblivious r-process and the equation of state(EOS) of a neutron star. The doubt on whether a KN is a potential source for lanthanide formation could also be verified from the spectral analysis.

To continue, the intrinsic luminosity variation of KN behaves like SN explosions. With the prevalence of BNS merge detection from next generation LIGO/Virgo(6-120 per year)[16], it could be extensively adopted as the standard candle for scientist to infer the luminosity distance from Earth. More investigations could be

accomplished including comparison between the redshift of KN and their host galaxies and corrections on cosmological constants like the Hubble parameter at large distance scale[17].

Regardless of the scientific importance of studying KN, its short emission timescale and multiple ejecta component appeals for an evaluation on LSST observation strategy. Hence, it is well-founded to establish a followup on gravitational wave induced by BNS merge.

3 Development on the Gravitational Wave Followup

3.1 LSST Targert-of-Opportunity Strategy

In order to search for the KN afterglow from LIGO's GW signal, we require a strategy that can orient the telescope to the localization region and filter out the possible host galaxies as soon as possible, together with short but consecutive exposure epoch to catch the rise and the peak of a KN, which has the greatest luminosity change. Therefore, the existing WFD and DDF strategy are poor candidates to complete the task. Yet, in 2018, the Gravitation Wave subgroup in the TVS Multiwavelength Characterization collaboration published a LSST Target-of-Opportunity(ToO) proposal and a strategy to search for GW optical transient was introduced in the paper[18]. In a brief summary, the ToO strategy suggested an utilization of the remaining few percent survey time. After receiving a trigger from LIGO/Virgo, if the sky condition is plausible for observation, the telescope would slew to the localization region and pile it up with into separate sections. In each section, exposures with different filters are made between a log-scale epoch ranging from 30 minutes to 8 hours, the larger the localization region, the fewer filters are used. Eventually, the ToO observation results in a repeating intra-night visits within the localization region.

In our GW followup, we develop a method which could evaluate the efficiency of ToO strategy. Similar evaluation has been done by Cowperthwaite et al. on 2018, but only for the WFD and DDF strategy and a prospect on ToO was made in the paper[19]. In our case, we would like to know how ToO actually differs from the baseline WFD proposal. The way to achieve it is to firstly inject a set of both ToO and WFD observation conditions into a software which could simulate a mixture of different optical transients including KN, and combine them with the two set of conditions to generate lightcurves for these transients. The reason of simulating a mixture of transients is to depict the realistic situation that there are millions of transients over the the localization region and one has to filter out those promising signals.

After that, lightcurves obtained by WFD and ToO strategy are passed into a classification program to receive filtered sets. They contain lightcurves which are classified to be KN with a certain percentage of confidence. Then the two sets, one from WFD and the other from ToO are ready to compare. By comparing the number of detected lightcurves in the two sets, two things could be understood. The first one, whether ToO observations helped to trigger more KN detection than WFD before the classification and filtering. And the second one, whether ToO observations helped to classify more true-positive KN detection than WFD. Finally, we could conclude if ToO is a more efficient proposal for GW followup or not.

3.2 Generate Simulation Library with OpSim and OpSimSummary

The Operation Simulator, OpSim, is a tool in the LSST pipeline for users to carry out simulation themselves. The simulator intake a set of user-defined parameters like the duration of survey, the strategy being used, and the region excluded from the survey, and return a set of observation conditions in SQlite table format. The observation conditions encompass the right ascen-

```
>>> table_name = 'kraken_2026.db'
>>> conn = sqlite3.connect('kraken_2026.db')
>>> cur = conn.execute("SELECT name from sqlite_master WHERE type = 'table';")
>>> for name in cur:
...     print(name[0])
...
Session
Field
TargetHistory
ObsHistory
SlewHistory
SlewInitialState
SlewFinalState
SlewActivities
SlewMaxSpeeds
TargetExposures
ObsExposures
ScheduledDowntime
UnscheduledDowntime
Proposal
ProposalField
ObsProposalHistory
TargetProposalHistory
Config
>>> cur = conn.execute("SELECT ra, dec from Field")
>>> cur.fetchall()
[(0.0, -90.0), (0.0, -85.272892), (0.0, -80.515486), (0.0, -75.741971), (0.0, -70.9
45.524505), (0.0, -40.051679), (0.0, -34.503126), (0.0, -28.931794), (0.0, -23.3831
5044), (0.0, 7.498197), (0.0, 12.307021), (0.0, 17.080554), (0.0, 21.837956), (0.0,
, 40.103692), (0.0, 42.871217), (0.0, 45.649902), (0.0, 48.440593), (0.0, 51.242702
```

Figure 3: Reading a kraken_2026 database, one of the lastest simulation done by LSST community with online source available. The database consists of several tables which comprises all the necessary observation conditions in a 10-year survey, the command afterwards was used to search for the sky position of each observation from the 'Field' table, which is an extensive number.

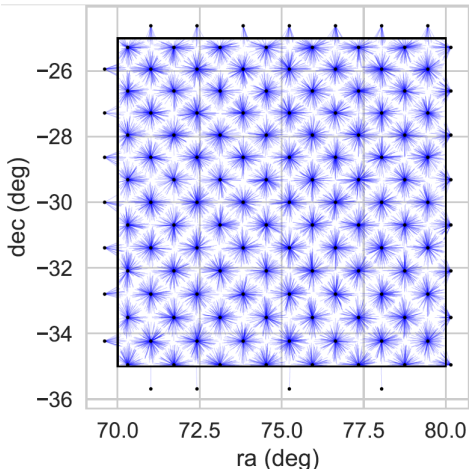

Figure 4: An brief picture on OpSimSummary mapping from[20], the reduce the number of sky positions handled by the transient simulator, observation pointing from OpSim output are grouped by choosing equally spaced field centres on sky, each blue line represents a mapping of OpSim pointing into the field centre. In this example, each field maps 64 observations into one. While for more realistic case which involves millions of observations, number of fields has to chosen carefully

sion(RA), declination(DEC), time of the observation begins and ends, sky brightness and other parameters. Figure 3 shows those table names which are available to be queried in one of the latest simulation output, using python SQlite.

Although OpSim is a promising tool to generate observation pointings, a complete 10 year simulation is a time-consuming process. Therefore, we decided to apply latest WFD simulation results accessible from online. Moreover, OpSim has default setup for WFD and DDF but not for ToO. Using OpSim to simulate ToO observation conditions would require customization on the simulator strategy. Instead, an approach of substituting WFD observation with ToO observations was employed and details will be discussed in following sections.

A 10-year survey over the sky involves extensive pointings, injecting them directly into a transient simulator without parallel execution support would be an exhaustive task. Thus, we firstly map the observations points and conditions into a single filed with shared RA, DEC. An example of point mapping is shown in figure 4.The process was carried out in OpSimSummary, a software which takes OpSim's SQlite output with user-defined, a piling strategy(Ditherfile) and a user-defined parameters(number of mapped fields etc.) into simulation library(simlib) format[20]. Figure 5 demonstrates a pontus_2489 simlib derived from the original OpSim database. One can see pointings with different RA, DEC are mapped into 5000 LIBID, each of them has 1500 observations. Sky conditions like sky signals and zero-point magnitudes are encoded into the simlib file as well.

It is worth notice that the number of piling field has to be set carefully. If the number of fields(LIBIDs) is too small, there are possibilities of multiple simulated events happening at the same field and at the same time, causing overlapping in the observations. Moreover, the RA, DEC for each field would be unrepresentative for the set of pointing as some of them could actually be far from the mapped sky position. Indeed, in reality, transients frequently happen

```
SURVEY: LSST    FILTERS: ugrizY  TELESCOPE: LSST
USER: azfar     HOST: des70.fnal.gov
NLIBID: 5000
NPE_PIXEL_SATURATE:   100000
PHOTFLAG_SATURATE:    1024
COMMENT: Total area corresponding to this simlib is 18236.4 sq degrees or a solid angl
COMMENT: This is a simlib corresponding to WFD in the OpSim Output /data/des70.a/data/
OpSimSummaryLatest/OpSimSummary/scripts/make_simlibs.py in version 1.25.3dev at time 2

COMMENT: PARAMS MINMJD: 59853.016794
COMMENT: PARAMS MAXMJD: 63501.3980903
COMMENT: PARAMS TOTAL_AREA: 18236.4346024
COMMENT: PARAMS SOLID_ANGLE: 5.5551356547

BEGIN LIBGEN
# --------------------------------------------
LIBID:            0
RA: +160.136719 DECL: -23.969482   NOBS:       1643 MWEBV:  0.00 PIXSIZE: 0.200
#                            CCD  CCD          PSF1 PSF2 PSF2/1
#     MJD      ID*NEXPOSE  FLT GAIN NOISE SKYSIG (pixels)  RATIO  ZPTAVG ZPTERR  MAG
S: 59925.3406      65073*2 Y  1.00  0.25  43.07 1.62 0.00 0.000  29.58  0.005 -99.000
S: 59925.3409      65074*2 Y  1.00  0.25  42.66 1.60 0.00 0.000  29.58  0.005 -99.000
S: 59925.3412      65075*2 Y  1.00  0.25  43.15 1.63 0.00 0.000  29.57  0.005 -99.000
S: 59944.3628      81771*2 Y  1.00  0.25  59.82 1.79 0.00 0.000  29.63  0.005 -99.000
S: 59947.3575      83767*2 Y  1.00  0.25  48.00 2.10 0.00 0.000  29.61  0.005 -99.000
S: 59948.2598      84545*2 Y  1.00  0.25  41.17 1.74 0.00 0.000  29.55  0.005 -99.000
S: 59948.2601      84546*2 Y  1.00  0.25  41.31 1.75 0.00 0.000  29.55  0.005 -99.000
S: 59950.3463      86913*2 z  1.00  0.25  43.67 1.73 0.00 0.000  30.52  0.005 -99.000
S: 59950.3620      86960*2 z  1.00  0.25  52.27 1.85 0.00 0.000  30.54  0.005 -99.000
```

Figure 5: Reading the generated simlib table to check if any abnormal parameter exists. This is a WFD output of the pontus_2489 database generated by Dr. Farrukh Azfar. In the simlib file, NLIBID tells the number of fields for point mapping, other mata parameters tells the earlist and latest time of all observation and the area covered by the survey. For WFD, it is 5.5 steradian. Each field(LIBID) tells the sky position of the middle point and number of observation being grouped into the field, which is varying with the field position as they are not evenly distributed. They are followed by detail conditions for each observation, which is preserved from the original OpSim output

at the same time interval. However, they are at different sky position. Therefore, small number of LIBIDs could not mimic the real situation on sky, while setting a too-large LIBID number would be equivalent of direct injection.

Another reason of generating the simlib file is to make the format be compatible with the software being used for combining observation pointings with simulated optical transients, which is discussed in next section.

3.3 SNANA and PLASTiCC simulation

The SuperNova ANAlysis(SNANA) software is an optical transient simulator developed in 2009 in the purpose of generating observations on different types of optical signal from supernova explosion[21]. Despite the fact that other more user-friendly simulators exist, like SNcosmo, they impose strict conditions in model creation. For example, SNcosmo only accepts models written in time-series-SED format and they has to be developed on top of existing source class. In contrast, SNANA provides sufficient freedom for model development such that we can adopt various KN models. Furthermore, SNANA supports simulations of a mixture of transient classes as long as the user prepare suitable input file, which was the case to be simulated.

In SNANA, user provides an observation summary in simlib format, a model and an input file which defines the simulating time interval, locations of models and simlib file, physical parameters for the transient models, interstellar conditions like k-correction and host galaxy correction, telescope specifications including bandpasses and search efficiency, triggering criteria and output parameters. Two models were chosen for our work, one is a model induced from the real photometric data of AT 2017gfo, the other one is a parametrized model suggested by Daniel Kasen in 2017[]. The following figure depicts a successful simulation of single type KN transient using the AT 2017gfo model.

```
 Optional SEARCHEFF_SPEC_FILE not specified -> skip.

 Optional SEARCHEFF_zHOST_FILE not specified -> Eff=100%

 Optional SEARCHEFF_zHOST_FILE not specified -> Eff=100%

************************************************************
   Fill comments for README doc-file

************************************************************
  clr_VERSION
       LCMERGE Version KNsim1 does not exist.
       SIM Version KNsim1 does not exist.
       PHOTOMETRY Version KNsim1 does not exist.

************************************************************
  Init SIMGEN_DUMP file
       open /home/andersonlai/SNANA/snana/KNSIM/SNDATA_ROOT/SIM/KNsim1/KNsim1.DUMP

************************************************************
   Begin Generating Lightcurves.
 Found Max dN/dz * wgt = 7.386863e+61 at z =    0.220
       Finished generating        1 of 11659 (CID=     1)
       Finished generating      100 of 11659 (CID=   100)
       Finished generating      200 of 11659 (CID=   200)
       Finished generating      300 of 11659 (CID=   300)
       Finished generating      400 of 11659 (CID=   400)
       Finished generating      500 of 11659 (CID=   500)
       Finished generating      600 of 11659 (CID=   600)
       Finished generating      700 of 11659 (CID=   700)
       Finished generating      800 of 11659 (CID=   800)
       Finished generating      900 of 11659 (CID=   900)
       Finished generating     1000 of 11659 (CID=  1000)
       Finished generating     1100 of 11659 (CID=  1100)
       Finished generating     1200 of 11659 (CID=  1200)
       Finished generating     1300 of 11659 (CID=  1300)
       Finished generating     1400 of 11659 (CID=  1400)
       Finished generating     1500 of 11659 (CID=  1500)
```

Figure 6: A successful simulation on lightcurves using parametrized model derived from AT2017gfo and the pontus_2489 WFD simlib. The first few lines tell whether a file that provides telescope configuration exists or not. One can see that in a complete WFD survey, there could be 10,000 or above KN event. Nevertheless, only a few of them would be detected. Still, all the simulated lightcurves will be logged into the .DUMP file

In order to achieve multiclass simulation, input templates were obtained from the PLASTiCC campaign. The PLASTiCC was originally raised in 2017 as an online challenge about a quick classification of mixed-classes lightcurves. We therefore implemented PLASTiCC simulation files in our work, figure 7 gives a brief summary of a successful simulation on a mixture of objects. After the PLASTiCC simulation, two data tables would be generated for each transient class. The file that ends with .DUMP tells information of all simulated afterglows, involving their object ids, positions, redshifts and the expected largest signal to be detected in each band. While the .FITS file contains the detected lightcurves by LSST, which could be resolved into different sets of photometic measurements for each lightcurves. By passing the simulated photometric data into the analysis code, lightcurves were illustrated.

```
                                                SUM-SNIa  :
  GENVERSION                                    NGEN      NWRITE  NSPEC
# ------------------------------------------  --------  --------  -----
LSST_WFD_KN-K14_minion_1016                        0         0       0
LSST_WFD_SALT2_minion_1016                         0         0       0


                                                SUM-NONIa :
  GENVERSION                                    NGEN      NWRITE  NSPEC
# ------------------------------------------  --------  --------  -----
LSST_WFD_KN-K14_minion_1016                     3320        20      11
LSST_WFD_SALT2_minion_1016                     18300     14036      27
```

Figure 7: The summary of a mixed simulation composing optical transients from type Ia supernova using the SALT2 model and Kilonova using Kasen's parametrized model. For technical convenience, they were put into the Non-Ia class but that didn't affect the simulation. Simulations were based on minion_1016 WFD simlib, another OpSim Output. From the summary, one can inspect that KN are much harder to detect compare to SNIa transients, a possible reason could be its strict tirggering criteria

Indeed, as one can see from figure 8 and 9, a multiband observation using WFD strategy could recover a KN-like lightcurve shape. However, if the observations are grouped according to bandpasses, the number of observations greatly reduces to 2 to 3 data points per band. Some bands even have missing observations. The consequence begins to emerge when the localization area is too large that observations can only be made with limiting bandpasses. It other

words, WFD strategy generates scarce photometric data to reproduce the lightcurve, especially when there are only 1 to 2 bands' data available for classification. Last but not least, an attempt of applying Cowperthwaite 2018 paper's statistics was made for a newer version of OpSim WFD run. Results were summarized in figure 10a, 10b, which are in good agreement with the paper's conclusion.

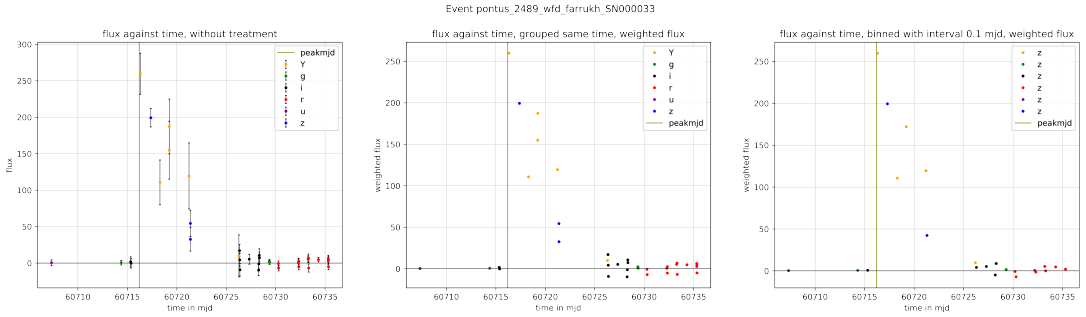

Figure 8: The multiband lightcurve of a detected KN event, it describes the variation of photon flux as time passes in modified julian day(MJD) scale. Each data point corresponds to one observation, while the color tells the bandpass used for that observation. The olive line indicates the theoretical mjd time for the KN to reach its peak magnitude, clear decaying shape is captured by multiband observation. The three lightcurve represents the same event, the right one is raw data, the middle one averages the photon flux of the same mjd and bandpass. The left one is binned photon flux of the same bandpass with 0.1mjd interval

3.4 Classifying Lightcurves with MOSFiT and RAPID

The goal of classification is to extract potential candidates which could be KN, two strategies were applied in our work. A traditional one is by fitting a model with varying parameters into the lightcurve and MOSTFiT was the software used for the fitting process[22]. It provides a 3-component KN model that corresponds to three types of r-process ejecta (red, blue and purple). Nonetheless, there are consequential drawbacks of applying the traditional method. To start with, there are not many KN lightcurve fitters. Although MOSFiT is one of them, there is only one model available for the fitting(the 3-component model) and 12 free parameters are involved for each band. Compare to the number of data points in WFD survey(0-3 points, section 3.3), the information is highly insufficient for the fitting. In this case, an overfit or an underfit of lightcurves would be the result, which is obviously deviate from the original data. Figure 11 gives the best illustration of the situation.

The next drawback is the duration of lightcurve fitting. A typical 12-parameter burning on SNANA's WFD photometry data with single core requires 30-40 minutes. Consider a situation of a multi-core parallel execution reduces the fitting time to 3 seconds, and a circular localization region of 20 - 30 square degrees that produces 50,000 triggered transients in the first sweep over the region is fitted by 10 different models. An aspiration of classification finishes at the beginning of second sweep is made, then a rough estimation could be done. Assuming the region is piled up into 4 sections, recall the FOV of LSST is 9.6 square degree. We further assume that transients are evenly distributed over the four fields. From ToO proposal, the first epoch would be 30 minutes. If exposure time for each band is 120 seconds and a full-band observation is considered. Then the time required for the first field in the first sweep, t_1, is:

$$t_1 = 30 + \frac{120}{60} \times 6 = 42 minutes$$

while the time required for fitting all transients, $t_1^{'}$, is:

$$t_1^{'} = \frac{3}{60} \times \frac{50000}{4} \times 10 = 6250 minutes$$

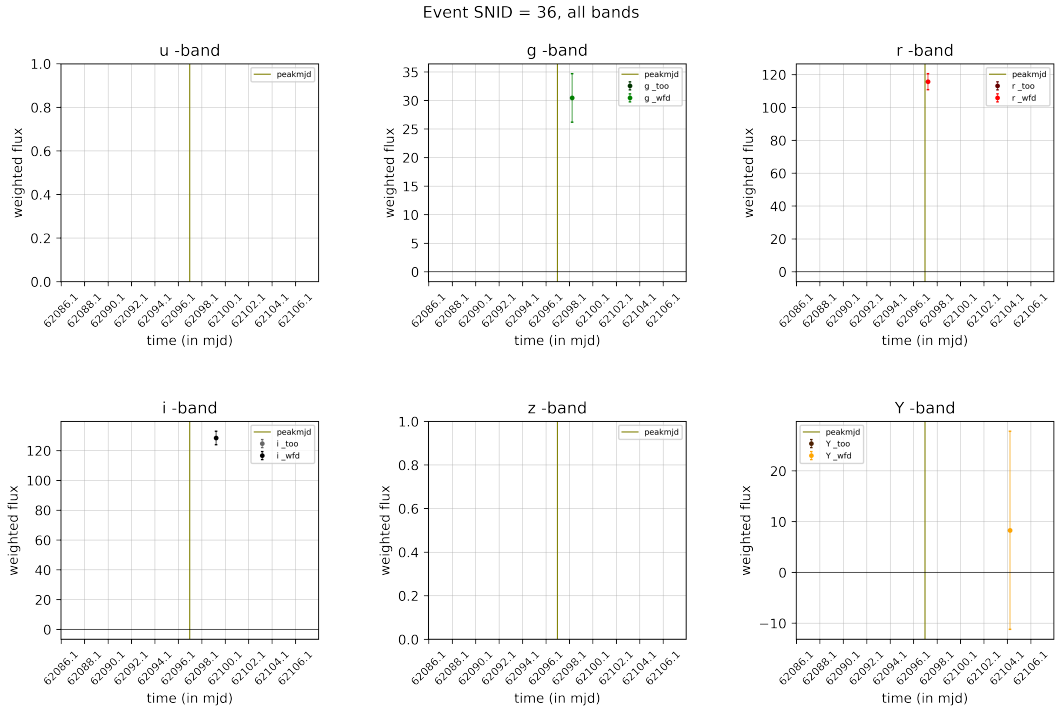

Figure 9: Another detected KN from simulation. However, observations are decomposed into different bands this time and the problem emerges. within the 6 bands, 4 of them have only one data and the rest has none. Although a multiband lightcurve reproduces the shape, the observations obtained with WFD strategy are actually insufficient for classification. Especially for some classifier which only use 2-3 bands observations(section 3.4)

From above estimation, it is obvious that even for an extremely efficient fitting process, a compilation time much longer than expectation is demanded. Thus, fitting photometric data with various model was considered to be a poor and time-inefficient option.

The alternative, which is considered to be a better choice in a sense of quick classification, relies on the software RAPID. RAPID is a program developed recently as the ultimate product of the aforementioned PLASTiCC campaign and based on the deep learning algorithm. By providing a set of lightcurves tagged with different classes of transients, a classifier is trained by the optical spectral difference of different classes[23]. After that, an unknown lightcurve is injected into the classifier and it returns a vector that includes the probability in each class at different time step. One of the injection result is presented with analysis in figure 12.

As long as the classifier is trained, differentiating unknown lightcurves would be a swift task. For example, classification on a set of 30 lightcurves could be completed in a few seconds. Regardless of the great advance in time efficiency, there are subtle flaws in RAPID. First of all, trained RAPID classifier's accuracy completely depends on the size and variety of the training set. The classifier being applied in LSST has to be carefully monitored such that when a promising new model arises, LSST has to generate sufficient samples and re-train the classifier with data set including those new samples. Moreover, RAPID makes use of the spectral difference between two bands in lightcurves as the key feature, a real photometric measurement which is lack in observations on certain band may induce substantial deviation on the prediction.

Bottom: The cumulative distribution of number of observations with SNR ¿ 5 after explosion, a SNR ¿ 5 criteria garuntee the data point is a promising one. Consider the black curve(all events), one can see for 200 above observations, only half of them has more than 4 promising observations over six band. It once again reveals the lack of vaild data point using WFD. The large deviation of red curve to black curve implies a significant number of observations lies on the rise rather than the post-peak-magnitude period

Figure 10: Figure 10. Above: It shows the cumulative distribution of the delayed time in mjd form. The delayed time counts from the peak magnitude time. The quicker the number reaches the total events number implies that the feature around the peak can be caught by the observation. Nevertheless, less than half of detected events uable to make the first observation within 0.5 days(typical time scale) after the peak magnitude reached.
Bottom: The cumulative distribution of number of observations with SNR ¿ 5 after explosion, a SNR ¿ 5 criteria garuntee the data point is a promising one. Consider the black curve(all events), one can see for 200 above observations, only half of them has more than 4 promising observations over six band. It once again reveals the lack of vaild data point using WFD. The large deviation of red curve to black curve implies a significant number of observations lies on the rise rather than the post-peak-magnitude period

3.5 OWSIM: Overwriting WFD Observations

One shall aware most of analysis and software run were implemented with WFD strategy. As describe in section 3.1, generating ToO observations is an arduous job and an approach of substituting existing WFD observation points was chosen. The Over-Write SIMulator(OWSIM) is a tool made for the job, it intakes a KN .DUMP file which tells the field and time interval where every simulated KN belongs to, a WFD OpSim output which was being used to generate the simlib for the first simulation and return an overwritten OpSim output with ToO observations substituted into it. Consequently, a new simlib file and SNANA simulation is repeated for the new output. By keeping the random

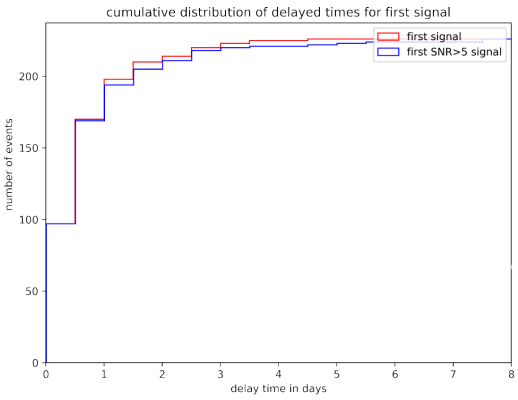

(a)

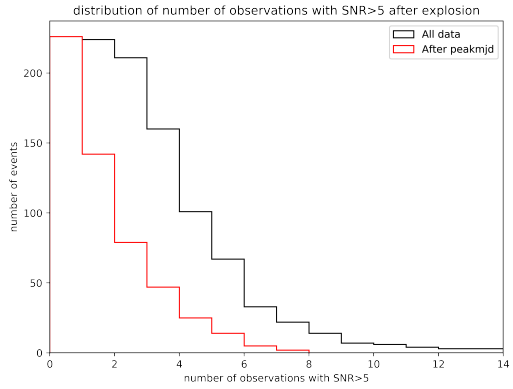

(b)

Bottom: The cumulative distribution of number of observations with SNR ¿ 5 after explosion, a SNR ¿ 5 criteria garuntee the data point is a promising one. Consider the black curve(all events), one can see for 200 above observations, only half of them has more than 4 promising observations over six band. It once again reveals the lack of vaild data point using WFD. The large deviation of red curve to black curve implies a significant number of observations lies on the rise rather than the post-peak-magnitude period

seed in SNANA, same KN can be simulated for both WFD and ToO observations. Eventually, lightcurves from the two strategies can be compared.

However, OWSIM is under development and require some debugging for use. Thus, ToO observations cannot be produced correctly by this time. Still, it is believed that the software could be put to use in near future.

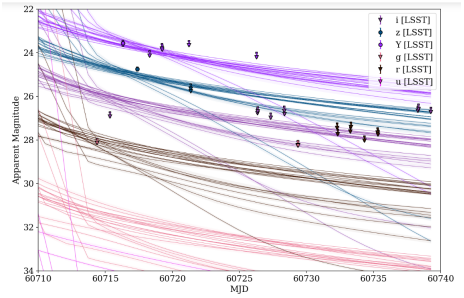

Figure 11: One of the MOSFiT result on fitting a lightcurve. Original data points can be seen clearly. There are many predicted lightcurves as MOSFiT presents all candidates which has the smallest optimization parameter. From data points, time at peak magnitude can be easily inferred(around mjd = 60718). Yet MOSFiT predicts a peak magnitude time much earlier than 60718(60710). That reflects the poor performance of traditional model fitting when fitting insufficient data against many free parameters

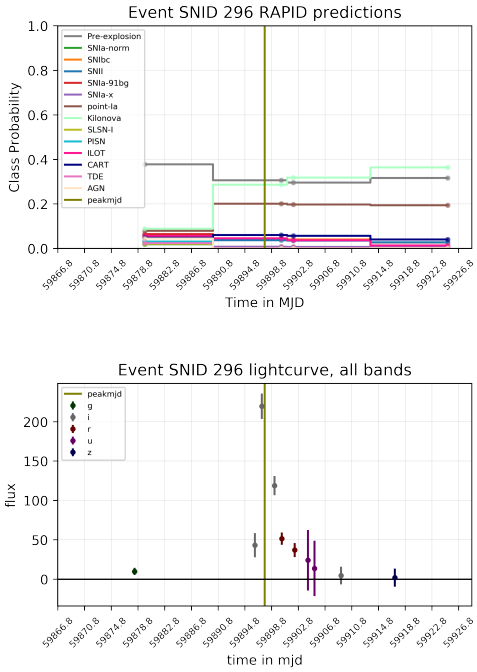

Figure 12: A demonstration of RAPID classification on one of the WFD detected lightcurve using their default pre-trained classifier. In RAPID, two bands of data were used(g and r in this case) and one can see from the top panel that the prediction varies with time as the magnitude of these bands changes in the bottom panel. Eventually, KNe comes out with the highest probability. Due to it's quick classification time, it is more likely to be the tool adopted by LSST compare to fitting method

4 Conclusions and Future Works

To summarize, a workflow on evaluating a certain GW followup strategy was basically set. Start with piling a WFD OpSim output into different fields and export to simlib format. Then, models of different optical transients and KN are blended with the simlib and telescope configurations in SNANA to obtain a mixture of lightcurves observed by WFD strategy. They are passed into the RAPID classifier afterwards to produce predictions on various transient classes. With the information of simulated KN from simulation, OWSIM can overwrite the WFD OpSim output and generate ToO observations. Above processes are then repeated and able to extend the analysis to ToO's results. A figure which summarizes the routine is delineate below.

Although intrinsic assumptions including each of the GW trigger with available observation conditions for companion KN must be searched by LSST and the mapping achieved by OpSimSummary is representative enough for those grouped pointings. Simple conclusions could be drawn from above process. For instance, whether a KN observed with ToO strategy gives higher confidence than WFD on predicting it into the correct class. The ultimate goal is to construct a strategy optimized for GW followup/KN search

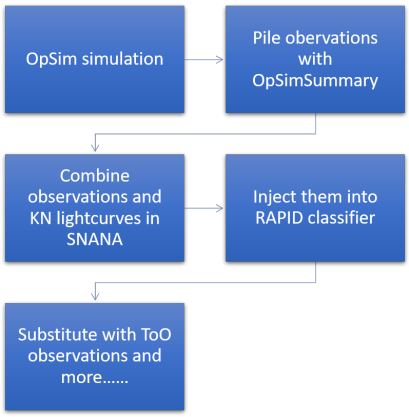

Figure 13: Figure that illustrate the workflow that has been walked through

by utilizing the feedback from this process.

Despite the future completion of OWSIM and followup workflow. Current cuts applied to trigger a LSST detection on optical transient is by maximizing the 5-σ depth. However, due to the short total exposure time on optical transients that rapidly decays with time, the 5-σ depth actually imposes a strict criteria on trigger. Therefore, in most cases, the sensitivity cannot reach to the theoretical 1 Gpc luminosity distance. In view of this, methods which could help to release the 5-σ trigger by considering other non-optical criteria might help to extend the searching range.

5 Acknowledgements

May I present my profound gratitude to:

The CN Yang Scholarship and Fung Scholarship for providing financial assistance for my travelling and living expenditure in this programe

Dr. Jeff Tsang for keeping up my work frequently and discussions which helped me to understand my task

Dr. Rahul Biswas for providing a detail picture and clarifying the ultimate goal of the project. At the same time, giving useful advises on software and simulation issues.

Dr. Farrukh Azfar for providing preliminary data for further analysis

The DESC_LSST group, including Eric Neilsen, James Annis, Marcelle Soares Santos and those who mentioned above.

References

[1] LIGO Scientific Collaboration and INTEGRAL et al. Virgo Collaboration, Fermi GBM. Multi-messenger observations of a binary neutron star merger. *The Astrophysical Journal Letters*, 848:59, 2017.

[2] Mochkovitch R. Daigne F. Duque, R. Neutron star merger afterglows: Population prospects for the gravitational wave era. *arXiv*, 2019.

[3] P. Anguita T. et al. LSST Science Collarboration, Marshall. Science-driven optimization of the lsst observaing strategy. *arXiv*, 2017.

[4] Liebendörfer M. Thielemann F. K. et al. Rosswog, S. Mass ejection in neutron star mergers. *Astronomy and Astrophysics*, 341:499.

[5] Kiuchi K. Kyutoku K. et al. Hotokezaka, K. Mass ejection from the merger of binary neutron stars. *Physical Review D*, 87, 2013.

[6] Sekiguchi Y. Nishimura N. et al. Wanajo, S. Production of all the r-process nuclides in the dynamical ejecta of neutron star mergers. *The Astrophyscial Journal Letters*, 789, 2014.

[7] D. Metzger, B. Welcome to the multi-messenger era! lessons from a neutron star merger and the landscape ahead. *arXiv*, 2017.

[8] Badnell N. R. Barnes J Kasen, D. Opacities and spectra of the r-process ejecta from neutron star mergers. *The Astrophysical Journal*, 774:13, 2013.

[9] Hotokezaka K. Tanaka, M. Radiative transfer simulations of neutron star merger ejecta. *The Astrophysical Journal*, 775, 2013.

[10] Kata D. Gaigalas G. et al. Tanaka, M. Properties of kilonovae from dynamical and post-merger ejecta of neutron star mergers. *The Astrophysical Journal*, 852:12, 2018.

[11] Metzger B. Branes J. et al. Kasen, D. Origin of the heacy elements in binary neutron-star mergers form a gravitational-wave event. *Nature*, 551:80.

[12] M. Bulla. Possis: predicting spectra, light curves, and polarization for multidimensional models of supernovae and kilonovae. *Monthly Notices of the Royal Astronomical Society*, 489:5037.

[13] D. Arnett, W. Analytic solutions for light curves of supernovae of type ii. *The Astrophysical Journal*, 237:541.

[14] D. Arnett, W. Type i supernovae. i. analytic solutions for the early part of the light curve. *The Astrophysical Journal*, 253:785.

[15] D. Martinez-Pinedo G. Darbha S. et al. Metzger, B. Electromagnetic counterparts of compact object mergers powered by the radioactive decay of r-process nuclei. *Monthly Noituces of the Royal Astronomical Society*, 406:2650.

[16] LIGO Scientific Collarboration and Virgo Collaboration et al. Gw170817: Observation of gravitational waves form a binary neutron star inspiral.

[17] F. Schutz, B. Determining the hubble constant from gravitational wave observations.

[18] Cowperthwaite P.-Doctor Z. et al. Margutti, R. Target of opportunity observations of gravitational wave events with lsst. *arXiv*, 2018.

[19] S. Villar-V. A. Scolnic D. M. Berger E. Cowperthwaite, P. Lsst target-of-opportunity observations of gravitational-wave events: Essential and efficient. *The Astrophysical Journal*, 874:16, 2019.

[20] Daniel S.-F. Hložek R. et al. Biswas, R. Enabling catalog simulations of transient and variable sources based on lsst cadence strategies. *arXiv*, 2019.

[21] Bernstein J-P. Cinabro D. et al. Kessler, R. Snana: A public software package for supernova analysis. *Publications of the Astronomical Society of the Pacific*, 121:1028, 2009.

[22] Nicholl M.-Villar V. A. et al. Guillochon, J. Mosfit: Modular open source fitter for transients. *The Astrophysical Journal Supplement Series*, 236:15, 2018.

[23] Narayan G.-Mandel K. S. et al. Muthukrishna, D. Rapid: Early classification of explosive transients using deep learning. *arXiv*, 2019.